ASTEROID RENDEZVOUS UNCERTAINTY PROPAGATION

Marc Balducci[*]

University of Colorado Boulder
Colorado Center for Astrodynamics Research
Boulder, CO 80301

Brandon A. Jones

The University of Texas at Austin
Aerospace Eng. and Eng. Mechanics
Austin, TX 78712

ABSTRACT

Most methods of propagating orbit uncertainty assume posteriori Gaussian distributions, require an intrusive implementation or suffer from the curse of dimensionality associated with high-dimensonal random inputs. Although Monte Carlo techniques avoid these drawbacks, the approach has a slow convergence rate. This paper considers the application of separated representations for orbit uncertainty propagation and discusses the theory behind their generation. The computation cost of a separated representation is largely linear with respect to dimension, thereby improving tractability when compared to methods that suffer from the curse of dimensionality. Generation of a separated representation requires the propagation of a small number of samples and yields an approximate solution, or surrogate, to a given stochastic differential equation describing the propagated orbit. This surrogate provides information on the moments and spatial density of possible solutions, as well as the sensitivity of the quantities of interest with respect to random inputs. This paper presents the case of spacecraft targeting an asteroid for a rendezvous, for which the initial conditions of each and the components of the interceptor maneuver are uncertain. Separated representations is used to estimate the probability of a successful rendezvous and analyze the resulting probability distribution functions.

Index Terms— non-Gaussian, curse of dimensionality, sensitivity analysis, separated representations

1. INTRODUCTION

Characterizing the variability of a system due to input and modeling errors is known as uncertainty quantification (UQ). Methods of UQ seek to estimate this variability in order to obtain a more complete understanding of an uncertain system. Typically, there is a trade-off between accuracy and computation time. One established, high accuracy approach is that of Monte Carlo (MC). Using this method, a large number of random variable realizations are propagated to a final state. From this state, statistical characteristics of the probability distribution function (PDF) can be calculated. MC has been proven effective when applied to the field of astrodynamics [1], but its performance comes at a high cost. The connergence rate of Monte Carlo is known to be inversely proportional to the square root of the number of realizations. This results in significant increases in sample size and computation costs in order to achieve incremental improvements in accuracy.

As an alternative, uncertainty mapping using the state transition matrix (STM) can be used to estimate a posterior PDF [2]. This method has extensive history within the astrodynamics community. Its relative requirement for computation time is low, but, due to its reliance on a linearization scheme, the approach is undesirable in the nonlinear regime of orbit propagation [3]. The unscented transform (UT) is an efficient approach that propagates uncertainty in a nonlinear fashion. However like the STM, the UT relies on Gaussian assumptions, which have been proven to be innacurate under cases of high variance, significant time between observations or both [3]. This paper considers the approach of surrogate methods in order to keep computation times low while maintaining high accuracy over long propogation times.

Methods such as Polynomial Chaos (PC) [4, 5, 6, 7, 8] and Gaussian Mixture Methods (GMM) [9, 10, 11] have been explored as alternatives to current approaches [6]. These UQ methodologies do not make Gaussian assumptions, but computation time remains a concern, as it increases quickly (up to exponential) with respect to the number of uncertain inputs or stochastic dimensions [12, 9]. In addition to these, state transition tensors (STT) are also being researched for the purposes of UQ [13, 14, 15]. Although STT are efficient and accurate for nonlinear propagation, derivation of complex partial derivatives or numerical methods are required for their approximation. Another technique currently undergoing research in the field of astrodynamics is that of differential algebra (DA). By replacing a typical implementation of computational algebra with an approximation based on Taylor polynomials, computation costs may be greatly reduced [16]. As applied to astrodynamics in [17, 18, 19] among others, DA provides an accurate and cost effective method to estimate PDFs in orbital environments. DA, however, is an intrusive method of uncertainty propagation, and therefore, existing and proven propagation techniques cannot be leveraged.

[*]Funded by NASA grant NNX15AP41H.

In addition to quanitifying the uncertainty of a system and the related statistics, it is often desirable to determine the relative effects that the random inputs have on the uncertainty of the system. This relationship, between the variability of the quantities of interest (QOIs) and the uncertain inputs, can be quantified with a sensitivity analysis [20]. Using an analysis of variance (ANOVA), sensitivity indices are produced. With these indices, random inputs with significant impact of QOIs can be identified, which could allow for justified dimension truncation. By identifying the inputs with larger effects on the solution uncertainty, it then becomes possible to prioritize dimension determination. With this priority in mind, the determination of these dimensions makes it possible to reduce output uncertainty by the largest possible ammount [20]. PC is able to generate such ANOVA based sensitivity indices analytically and has been shown to be efficient [21], however, this low computation cost lies in the assumption of a low dimension problem or low polynomial degree. By assuming low stochastic dimension, the scope of a sensitivity analysis may become limited.

As a potential solution to the trade-off between accuracy and computation, we propose the approach of *separated representations* (SR) for propagating uncertainties associated with the initial state of objects in space and other parameters to a future time. SR provides a surrogate model by decomposing a multivariate function of inputs into a sum of products of univariate functions of those inputs. This low rank decomposition can efficiently quantify the response of a system to a set of inputs. SR has been shown to significantly reduce computation times for high-dimension stochastic systems [22, 23, 24, 25, 12, 26, 27, 28, 29], while making no assumptions of a Gaussian *a posteriori* distribution. Since it was first applied to astrodynamics by [30], SR has also been used to produce a direct solution of the Fokker-Planck equation for perturbed Keplerian mechanics [31]. Crucially, the theory of SR predicts that the computational complexity remains linear with respect to the number of random inputs. This has been demonstrated by Beylkin, et al [32]. By maintaining a low cost with respect to stochastic dimension, the available suite of random inputs can be utlized without significantly increasing computation time. In addition to this, SR is capable of producing moments analytically via an analysis of available coefficients [12].

This paper presents tests and numeric examples which consider the use of SR methods for the propagation of the multivariate state PDF of an asteroid and an intercepting spacecraft without a posterior Gaussian assumption. The results of numeric tests are used to quantify the probability of a sucessful rendezvous. Section 2 introduces the setup for rendezvous problem. Section 3 then presents the method of SR and an overview of implementation. Following these sections, Section 4 examines experimental tests and associated results for the presented rendezvous problem, while Section 5 concludes the paper with a summary for future work.

2. PROBLEM SETUP

To describe the rendezvous scenario, this work examines the state of the target asteroid 2006 DN $\boldsymbol{q}_{DN}$ and an interceptor $\boldsymbol{q}_{int}$. Both of these states consist of the object's heliocentric Cartesian position and velocity components. These values are considered the QOIs. By propagating an initial collection of QOIs $\boldsymbol{q}_0 \in \mathbb{R}^M$, the state of the heliocentric system can be found at a later time, $\boldsymbol{q} \in \mathbb{R}^M$, where M denotes the dimension of the QOI. It should be noted that the particular elements of $\boldsymbol{q}_0$ and $\boldsymbol{q}$ are not required to be related on a one-to-one basis. For instance, the initial QOIs could be the orbital states of our objects, while the final QOI could be time of flight. In this case, $\boldsymbol{q} = [\boldsymbol{q}_{DN}, \boldsymbol{q}_{int}]^{\mathrm{T}}$ and $M = 12$.

In order for the interceptor to rendezvous with the asteroid, a maneuver is required. This burn is computed using the initial conditions of both objects as inputs into a Lambert solver and occurs at the initial time t_0. The uncertainties in the probelm results from inaccuracies in the initial states of both the asteroid and interceptor, as well as errors in the aforementioned maneuver. By assuming the state $\boldsymbol{q}$ depends on d random variables $\boldsymbol{\xi} \in \mathbb{R}^d$, we characterize the uncertainty in the initial state and the burn direction and magnitude. In this paper, d is the stochastic dimension referred to in Section 1 and the following sections.

The state of both objects at the propagated time t is denoted as $\boldsymbol{q}(t, \boldsymbol{\xi})$ and satisfies a set of ODEs

$$\boldsymbol{\mathcal{F}}\left(t, \boldsymbol{\xi}; \boldsymbol{q}\right) = \boldsymbol{0} \tag{1}$$

describing the temporal evolution of the each state. In this scenario, $t \in [t_0, t_f]$ is the temporal variable and the initial condition

$$\boldsymbol{q}(t_0, \boldsymbol{\xi}) = \boldsymbol{q}_0(\boldsymbol{\xi}) \tag{2}$$

is considered. For the interest of a cleaner presentation, the temporal dependence of $\boldsymbol{q}$ is restricted to a fixed instance of t and the short notation of $\boldsymbol{q}(\boldsymbol{\xi})$ is adopted.

The components of $\boldsymbol{\xi}$, denoted by ξ_i, are defined as independent, standard Gaussian random variables when applied to the initial states of both the asteroid and the interceptor, i.e., $\boldsymbol{\xi} \sim \mathcal{N}\left(\boldsymbol{0}, \boldsymbol{I}_{12\times 12}\right)$, where $\boldsymbol{I}_{12\times 12}$ is the 12×12 identity matrix. In order to model the maneuver, a combination of Gaussian and uniform random inputs is employed. Since twelve other random inputs have been defined, the following maneuver random inputs begin with a subscript of thirteen. Given the nominal maneuver $\overline{\Delta \boldsymbol{V}}$ described in Cartesian coordinates, the sampled maneuver vector is calculated as

$$\Delta \boldsymbol{V}(\xi_{13}, \xi_{14}, \xi_{15}) = \overline{\Delta \boldsymbol{V}} + \delta \Delta \boldsymbol{V}(\xi_{13}, \xi_{14}, \xi_{15}) \tag{3}$$

$$\delta \Delta \boldsymbol{V}(\xi_{13}, \xi_{14}, \xi_{15}) = \dots$$
$$\boldsymbol{Q}(\xi_{14}, \xi_{15}) \otimes (\xi_{13}\sigma_{mag}\overline{\Delta \boldsymbol{V}}) \otimes \boldsymbol{Q}^*(\xi_{14}, \xi_{15}), \tag{4}$$

where $\boldsymbol{Q}$ is the quaternion defining the transformation from the maneuver error frame to the inertial frame, $\boldsymbol{Q}^*$ is the conjugate of this quaternion, σ_{mag} is the error of the maneuver burn magnitude as a percent from the nominal, and $\otimes$ is the quaternion multiplication operator. As previously stated, a hybrid strategy of Gaussian and uniform variables is employed, i.e., $\xi_{13}, \xi_{14} \sim \mathcal{N}(0,1)$ and $\xi_{15} \sim \mathcal{U}(-1,1)$. In this application, $\delta\Delta\boldsymbol{V}$ is the error of the maneuver burn. In order to calculate the direction of this error, the angles $\theta(\xi_{14})$ and $\phi(\xi_{15})$ are embedded within the quaternion $\boldsymbol{Q}$. As seen in Figure 1, the angle $\theta(\xi_{14})$ defines the deviation of the maneuver relative to the nominal maneuver, while $\phi(\xi_{15})$ is a rotational error about this nominal direction. In this application, the rotational angle is distributed as $\phi(\xi_{15}) \sim \mathcal{U}(-\pi,\pi)$. For an application with additional details, the reader is recommended the paper by Jones, et al. [6].

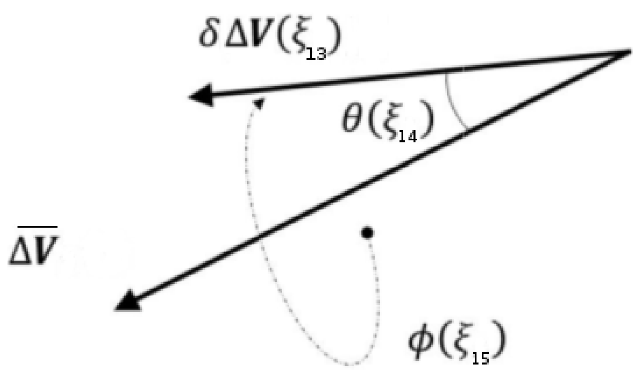

Fig. 1. Maneuver execution error including angle errors. Adapted from an image found in [33]

In a typical application of MC, the statistics of $\boldsymbol{q}(\boldsymbol{\xi})$, such as the mean and standard deviation (STD), are estimated by evalulating a large number N of realizations of $\boldsymbol{q}(\boldsymbol{\xi})$, $\{\boldsymbol{q}(\boldsymbol{\xi}_j)\}_{j=1}^N$. These values are propagated from the initial state condition $\{(\boldsymbol{\xi}_j, \boldsymbol{q}_0(\boldsymbol{\xi}_j))\}_{j=1}^N$, where $\boldsymbol{\xi}_j$ is an arbitrary sample of $\boldsymbol{\xi}$. For notation purposes, the jth sample of ξ_i is given as $\xi_{i,j}$. The joint PDF of $\boldsymbol{q}$ may also be approximated using a sufficiently large number of realizations of $\boldsymbol{q}$.

The construction of SR relies on using random samples of $\boldsymbol{\xi}$, $\{\boldsymbol{\xi}_j\}$ and the corresponding realizations $\{\boldsymbol{q}(\boldsymbol{\xi}_j)\}$ from black box propagations, where the distance between $\boldsymbol{q}(\boldsymbol{\xi})$ and the SR approximation $\hat{\boldsymbol{q}}(\boldsymbol{\xi})$ is minimized at the samples $\{\boldsymbol{\xi}_j\}$ using a regression approach. As leveraged throughout this paper, we define the data-dependent inner product of two vectors $\boldsymbol{q}(\boldsymbol{\xi}), \boldsymbol{r}(\boldsymbol{\xi}) \in \mathbb{R}^M$ as

$$\langle \boldsymbol{q}, \boldsymbol{r} \rangle_D = \frac{1}{N} \sum_{j=1}^{N} \langle \boldsymbol{q}(\boldsymbol{\xi}_j), \boldsymbol{r}(\boldsymbol{\xi}_j) \rangle_2 , \qquad (5)$$

where $\langle \cdot, \cdot \rangle_2$ denotes the standard Euclidean inner product. The inner product in (5) induces the norm

$$\|\boldsymbol{q}\|_D = \langle \boldsymbol{q}, \boldsymbol{q} \rangle_D^{1/2} , \qquad (6)$$

which is used within this presentation.

3. SEPARATED REPRESENTATIONS

This presentation of SR is a modification of that which is shown in the papers [34, 30, 12, 32]. For the sake of brevity, the reader is referred to these references for more details. As a surrogate method, the separable approach is that of approximating a multivariate scalar function $q(\boldsymbol{\xi})$ with a sum of products of univariate functions. With the simplest form of SR, the estimation of the scalar function may be formulated as a product of separate, univariate functions

$$q(\boldsymbol{\xi}) \approx \hat{q}(\boldsymbol{\xi}) = \prod_{i=1}^{d} u_i(\xi_i), \qquad (7)$$

with $\hat{q}(\boldsymbol{\xi})$ being the separated approximation of $q(\boldsymbol{\xi})$. The univariate functions of Eq. 7 are calculated so that the difference between $\hat{q}(\boldsymbol{\xi})$ and $q(\boldsymbol{\xi})$ is as small as possible. As a relatively simple approximation, this method is inflexible and may not achieve a desired accuracy. Therefore, a sum of seperable functions is often considered, taking the form of

$$q(\boldsymbol{\xi}) \approx \hat{q}(\boldsymbol{\xi}) = \sum_{l=1}^{r} s^l \prod_{i=1}^{d} u_i^l(\xi_i) . \qquad (8)$$

By expanding the approximation into a sum with *separation rank* r, the unknown univariate functions, or *factors* are now indexed from $1, \ldots, r$, i.e., $\{u_i^l(\xi_i)\}_{l=1}^r$, $i = 1, \ldots, d$, and are normalized by the constants $\{s^l\}_{l=1}^r$ such that each factor has unit norm.

These factors are approximated by unknown constants and a known polynomial basis in ξ_i,

$$u_i^l(\xi_i) \quad \approx \quad \sum_{p=0}^{P} c_{i,p}^l \psi_p(\xi_i), \qquad (9)$$

where $\psi_p(\xi_i)$ is a polynomial of degree p. This approach discretizes the univariate functions and allows for an optimization problem which is focused on finding the unknown coefficients $\boldsymbol{c}_i^l = [c_{i,1}^l, \ldots, c_{i,P}^l]$ along an individual direction i and rank l via

$$\min_{\{\boldsymbol{c}_i^l\}} \|q - \hat{q}\|_D^2 . \qquad (10)$$

3.1. Polynomial Basis

As explained in [35], the choice of the polynomial basis is based on establishing orthonormality between the basis of each random input direction i and the corresponding probability density function of ξ_i. Applied with respect to PC, this same approach is used when choosing the polynomial basis for SR. In the case of a normal Gaussian distribution, Hermite polynomials are chosen. However, due to the anglular property of the rotaion $\phi(\xi_{15})$, the corresponding polynomial is that of the Fourier basis

$$\psi_p(\xi_i) \in \{\cos(p\pi\xi_i), \sin(p\pi\xi_i)\}, \qquad (11)$$

and thus require two separate unknown coefficients. Applied to astrodynamic estimation using PC in [36], the Fourier basis is the appropriate choice for the case of $\phi(\xi_{15})$ as it is orthogongal with respect to the circular uniform distribution in question [36].

3.2. Vector-Valued Function Estimation

In the case of the rendezvous application, it is desirable to esimate the vector-valued QOI via SR simultaneously. For this case, the SR approximation of $\boldsymbol{q}(\boldsymbol{\xi}) \in \mathbb{R}^M$ is determined by

$$\boldsymbol{q}(\boldsymbol{\xi}) \approx \hat{\boldsymbol{q}}(\boldsymbol{\xi}) = \sum_{l=1}^{r} s^l \, \boldsymbol{u}_0^l \prod_{i=1}^{d} u_i^l \left(\xi_i\right). \tag{12}$$

In this formulation, the definitions and process of approximating $u_i^l(\xi_i)$ remain the same as previously determined in Eq. 8. The vector-valued definition of SR differs most significantly from Eq. 8 due to the vector of deterministic factors $\boldsymbol{u}_0^l = [u_{0,1}^l, \ldots, u_{0,M}^l]^{\mathrm{T}} \in \mathbb{R}^M$. These deterministic factors are used to to enable vector-valued approximations for $\boldsymbol{q}(\boldsymbol{\xi})$ by solving the optimization problem

$$\min_{\{\boldsymbol{c}_i^l\},\{\boldsymbol{u}_0^l\}} \|\boldsymbol{q} - \hat{\boldsymbol{q}}\|_D^2 . \tag{13}$$

Due to the addition of the deterministic factor vector, the set of scalars s^l are now normalization constants such that both $u_i^l(\xi_i)$ and $\boldsymbol{u}_0^l$ have unit norm.

3.3. SR Construction Overview

The work in this paper utilized a process of constructing an SR solution which in non-intrusive. Therefore, this method considers an existing ODE solver as a black box, propagating samples which are used to generate an SR solution. These samples are organized as a set $\{(\boldsymbol{\xi}_j, \boldsymbol{q}(\boldsymbol{\xi}_j))\}$ of N random samples, and their generation does not require any alterations of the solvers for (1). With this in mind, the non-intrusive SR process may be broken down into the following steps:

1. Generate a set of independent, random realizations $\{\boldsymbol{\xi}_j\}_{j=1}^N$ based on appropriate probability density functions

2. Using the *a priori* state distribution, generate the set of samples $\{\boldsymbol{q}_0(\boldsymbol{\xi}_j)\}_{j=1}^N$ at the epoch time.

3. Using a black box ODE solver, propagate N samples to the time of interest in order to get $\{\boldsymbol{q}(\boldsymbol{\xi}_j)\}_{j=1}^N$.

4. Use the training data $\{(\boldsymbol{\xi}_j, \boldsymbol{q}(\boldsymbol{\xi}_j))\}_{j=1}^N$ to generate the SR approximation.

3.4. Generating the SR Approximation

The process of step 4 in the previous section produces an SR solution, which is done with a method known as alternating least squares (ALS). This approach keeps the computation cost of SR low when compared to methods such as PC, due to the nonlinear optimization problem being reduced down into a series of linear least squres regression problems [32].

The overall approach of ALS involves estimating the coefficients $\{\boldsymbol{c}_i^l\}$ for one direction of interest $k = 1, \ldots, d$ at a time, given a pre-selected basis $\{\psi_p(\xi_i)\}$. To update these values, the unknown coefficients can be organized as

$$\boldsymbol{z} = \left[\left(\boldsymbol{c}_k^1\right)^{\mathrm{T}} \quad \cdots \quad \left(\boldsymbol{c}_k^r\right)^{\mathrm{T}} \right]^{\mathrm{T}}, \tag{14}$$

while the training samples $\boldsymbol{q}(\boldsymbol{\xi})$ are held in the data matrix

$$\boldsymbol{h} = \left[\boldsymbol{q}(\boldsymbol{\xi}_1)^{\mathrm{T}} \quad \cdots \quad \boldsymbol{q}(\boldsymbol{\xi}_N)^{\mathrm{T}} \right]^{\mathrm{T}} \in \mathbb{R}^{MN}. \tag{15}$$

An estimate of these values can be found as a solution to the problem

$$\{\boldsymbol{c}_k^l\}_{l=1}^r = \underset{\{\boldsymbol{c}_k^l\}_{l=1}^r}{\arg\min} \; \|\boldsymbol{q} - \hat{\boldsymbol{q}}\|_D^2 . \tag{16}$$

To do this, we solve via the the normal equation

$$\left(\boldsymbol{A}^{\mathrm{T}}\boldsymbol{A}\right) \boldsymbol{z} = \boldsymbol{A}^{\mathrm{T}}\boldsymbol{h}, \tag{17}$$

while $\boldsymbol{A}$ has the block matrix format

$$\boldsymbol{A} = \begin{bmatrix} \boldsymbol{A}_{11} & \cdots & \boldsymbol{A}_{1r} \\ \vdots & \ddots & \vdots \\ \boldsymbol{A}_{N1} & \cdots & \boldsymbol{A}_{Nr} \end{bmatrix}, \tag{18}$$

where the (j, l) block of $\boldsymbol{A}$, $\boldsymbol{A}_{jl} \in \mathbb{R}^{M \times P}$, is given by

$$\boldsymbol{A}_{jl} = s^l \left[\boldsymbol{u}_0^l \, \psi_1(\xi_{k,j}) \cdots \boldsymbol{u}_0^l \, \psi_P(\xi_{k,j}) \right] \prod_{i \neq k} u_i^l \left(\xi_{i,j}\right). \tag{19}$$

The vector $\boldsymbol{z}$ is solved for each direction in alternation until all directions $k = 1, \ldots, d$ have gone through the least squares process. After this has been completed, the best estimate of the deterministic factors $\{\boldsymbol{u}_0^l\}$ is found. Estimating these values is similar to the process outlined in Eqs. 14 - 19, with appropriate modifications. For more detail, readers are encouraged to examine the references [30, 34].

4. NUMERIC RESULTS

For this paper, the problem setup of Section 2 is examined in order to determine the chance of success for a rendezvous between an asteroid and an interceptor with uncertain initial conditions. In addition to this, the spacecraft undergoes an initial maneuver with errors in the magnitude and direction of the burn. The maneuver is implemented as occuring instantaneously at the beginning of the scenario, April 11, 2019 at

00:00:00 UTC. This scenario considers only a single burn at the epoch time. To determine this chance of close contact, this paper considers the distance between realizations of the asteroid and interceptor at the final time of flight by using a sampling based method, i.e.,

$$\delta q(\boldsymbol{\xi}) = \|\boldsymbol{q}_{DN} - \boldsymbol{q}_{int}\|, \tag{20}$$

where $\delta q(\boldsymbol{\xi})$ is the distance between the two objects. Each sample is propagated for 1088 days using a Dormand-Prince 5(4) ODE integrator, with a nominal arrival time of April 3, 2022. This integrator uses a tolerance of 10^{-13} and two body point mass dynamics of the sun. By defining a successful rendezvous of a propagation as resulting in an asteroid-interceptor distance of $\delta q(\boldsymbol{\xi}) < 400$ km, the ratio of successful to unsuccesful propagations can be calculated when analyzing a large number of samples [37].

4.1. Initial Conditions

Initial state uncertainty STDs for 2006 DN were found usir the JPL Small-Body Database Browser[1]. These values can t found in Table 1 along with initial conditions of the state ar consist of values for classic Keplerian elements such as sem major axis, inclination and mean anomaly. By using patche

Table 1. Parameters for Initial State Gaussian Distribution f 2006 DN

	Mean	STD
a (AU)	1.38013	$3.0097e-04$
e	0.27859	$1.5878e-04$
inc (deg)	0.26764	$1.3974e-04$
ω (deg)	101.24110	$4.3343e-03$
Ω (deg)	96.62356	$6.6975e-03$
M (deg)	8.69171	0.72173

conics and a Lambert solver, the nominal components for the interceptor maneuver were found. Table 2 includes the random inputs and their associated STDs. Position and velocity components are given in heliocentric Cartesian coordinates.

4.2. Analysis

Using $r = 8$, $P = 3$ and 1200 training samples, an SR solution for the heliocentric states of both objects was found. As a vizualization aid, the distributions of the SR-based PDFs and MC runs of 1,000,000 samples are created and plotted in Figures 2 and 3. The multivariate PDF is evaluated by using independent sets of random variables and the appropriate uncertainties.

In these figures, the red line is a fit for the center of the MC bins, while the black bins represent the results evaluated

[1]http://ssd.jpl.nasa.gov/sbdb.cgi

Table 2. Random inputs and associated STDs for the interceptor

	Mean	STD
x (AU)	-0.93808	$1.33691e-09$
y (AU)	-0.35197	$1.33691e-09$
z (AU)	$1.9736e-05$	$1.33691e-09$
$\dot{x}$ (km/s)	9.99105	$8e-03$
$\dot{y}$ (km/s)	-28.00263	$8e-03$
$\dot{z}$ (km/s)	$2.1797e-04$	$8e-03$
$\overline{\boldsymbol{\Delta V}}_x$ (km/s)	1.51305	0.01513
$\overline{\boldsymbol{\Delta V}}_y$ (km/s)	-3.48573	0.03485
$\overline{\boldsymbol{\Delta V}}_z$ (km/s)	-0.05830	$5.830e-04$
θ (deg)	0	1
ϕ (deg)	0	π

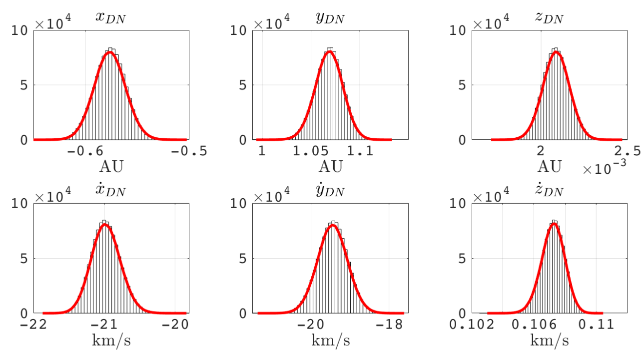

Fig. 2. Histograms of the final state PDF for asteroid DN

with the SR solution. Qualitatively, the fit is good, even considering the extended tails or sharp peaks of a non-Gaussian distribution. Although some of the MC data may appear to be Gaussian, applying the Jarque-Barre test to each QOI yields the detection of a non-Gaussian distribution in all but the y-component of 2006 DN's velocity. By taking advantage of the properties of SR, analytic results for the first and second moment are calculated. These numeric results and a comparison of the MC and SR approach are included in Table 3. In this table, the accuracy of the estimation is determined by a relative residual. Considering some value λ, the relative residual may be defined as

$$\epsilon_{rel} = \left| \frac{\lambda - \hat{\lambda}}{\lambda} \right|. \tag{21}$$

The results of Table 3 indicate at least three or more digits of precision in the first and second moments of the state PDFs. For this test case, a sensitivity analysis is also considered. Discussed in Section 1 and elaborated upon in [36], the sensitivity of each QOI with respect to all random inputs is calculated. Table 4 includes the results of a total sensitivity

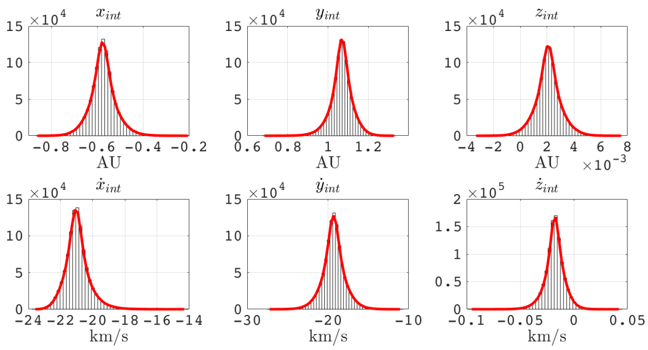

Fig. 3. Histograms of the final state PDF for the interceptor

Table 3. Agreement between SR- and PC-based mean and STD

	Rel. Mean	Rel. STD
x_{DN}	3.5e-05	7.9e-04
y_{DN}	1.6e-05	1.4e-03
z_{DN}	4.4e-05	9.4e-04
$\dot{x}_{DN}$	1.7e-06	2.6e-04
$\dot{y}_{DN}$	1.0e-05	9.1e-04
$\dot{z}_{DN}$	7.9e-06	4.2e-03
x_{int}	6.5e-05	5.7e-04
y_{int}	9.9e-06	2.2e-03
z_{int}	1.0e-04	4.3e-04
$\dot{x}_{int}$	3.6e-05	4.7e-04
$\dot{y}_{int}$	3.2e-05	2.2e-04
$\dot{z}_{int}$	5.9e-04	2.0e-03

analysis for the asteroid 2006 DN. The random inputs associated with the interceptor's state are not included, as they are calculated to be zero. The current approach, by determining these indices with 1,000,000 samples, produces one digit of precision. Therefore, many values are approximately zero. As seen in Table 4, the mean anomaly has the most significant contribution of uncertainty to the QOIs when considering the PDF of asteroid 2006 DN. In addition to the asteroid, sensitivities for the intercepting spacecraft are also provided. Table 5 includes the indices, which, in turn, leaves out the contributions of the random inputs associated with 2006 DN. It should be noted that other than impacting the QOIs the most, the random inputs of $|\Delta \boldsymbol{V}|$ and ϕ are also highly correlated. This is determined by the sum of the indices being larger than one. Inutitively, this makes sense, as the total impact of the maneuver is determined by the magnitude and direction of the burn.

Using these PDFs and Eq. 20, the probability of rendezvous success between the asteroid and the interceptor is calculated. Comparing the distance between each of the 1,000,000 samples, the histogram in Figure 4 is produced,

Table 4. Sensitivity indices for 2006 DN

	Quantities of Interest					
Inputs	x_{DN}	y_{DN}	z_{DN}	$\dot{x}_{DN}$	$\dot{y}_{DN}$	$\dot{z}_{DN}$
a	~ 0	~ 0	~ 0	~ 0	~ 0	~ 0
e	~ 0	~ 0	~ 0	~ 0	~ 0	~ 0
inc	~ 0	~ 0	~ 0	~ 0	~ 0	~ 0
ω	~ 0	~ 0	~ 0	~ 0	~ 0	~ 0
Ω	~ 0	~ 0	~ 0	~ 0	~ 0	~ 0
M	0.9	0.9	0.9	0.9	0.9	0.9

Table 5. Sensitivity indices for the interceptor

	Quantities of Interest					
Inputs	x_{int}	y_{int}	z_{int}	$\dot{x}_{int}$	$\dot{y}_{int}$	$\dot{z}_{int}$
x_{int}	~ 0	~ 0	~ 0	~ 0	~ 0	~ 0
y_{int}	~ 0	~ 0	~ 0	~ 0	~ 0	~ 0
z_{int}	~ 0	~ 0	~ 0	~ 0	~ 0	~ 0
$\dot{x}_{int}$	~ 0	~ 0	~ 0	~ 0	~ 0	~ 0
$\dot{y}_{int}$	~ 0	~ 0	~ 0	~ 0	~ 0	~ 0
$\dot{z}_{int}$	~ 0	~ 0	~ 0	~ 0	~ 0	~ 0
$\|\Delta \boldsymbol{V}\|$	0.8	0.9	0.9	0.9	0.8	0.8
θ	~ 0	~ 0	~ 0	~ 0	~ 0	~ 0
ϕ	0.8	0.8	0.9	0.8	0.8	0.9

as well as and empirical approximation of the cumulative distribution function (CDF), $F(\boldsymbol{\xi})$, in Figure 4. The scale

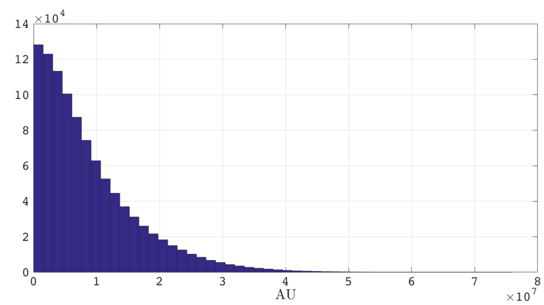

Fig. 4. Histogram of the distance between 2006 DN and an interceptor

of the separation of the two objects should be noted. With the current approach, the minimum distance found is approximately $4.4e03$ km. This places any potential approach of 2006 DN well outside the considered sphere of a successful rendezvous. In this case, it is assumed that the volumes of the PDFs are large in comparison to the desired distance. Therefore, without a TCM or alternate means of probability calculation, the probability of a mission success is approximately zero.

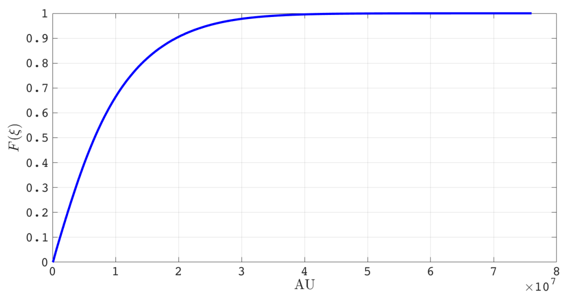

Fig. 5. CDF of the distance between 2006 DN and an interceptor

5. CONCLUSIONS AND FUTURE WORK

While the probability of a rendezvous in this scenario is calculated to be zero, the PDFs of both 2006 DN and an intercepting spacecraft are accurately estimated using the approach of separated representations. In this case, the methodology of SR requires significantly less propagated samples than a comparable MC run. With this data now availale, more work may be done to detect or increase the chances of a mission success. This includes adding a TCM to the mission design or implementing an all-to-all methodology for computing statistics from a large sample set. By adding a TCM, the analysis of this scenario can include the quantification of the uncertainty in the QOIs as a function of the TCM errors. This approach also allows for optimization under uncertainty with respect to TCM design, thus reducing the *a posteriori* spread of the PDFs.

6. REFERENCES

[1] Chris Sabol, Christopher Binz, Alan Segerman, Kevin Roe, and Paul W Schumacher Jr, "Probability of collision with special perturbations dynamics using the monte carlo method," in *AAS/AIAA Astrodynamics Specialist Conference, Girdwood, AK*, 2011.

[2] Bob Schutz, Byron Tapley, and George H Born, *Statistical orbit determination*, Academic Press, 2004.

[3] J. L. Junkins, M. R. Akella, and K. T. Alfriend, "Non-gaussian error propagation in orbital mechanics," *Journal of Astronautical Sciences*, vol. 44, no. 4, pp. 541–563, Oct.-Dec. 1996.

[4] R.G. Ghanem and P.D. Spanos, *Stochastic Finite Elements: A Spectral Approach.*, Springer-Verlag, New York, 1991.

[5] D. Xiu, *Numerical Methods for Stochastic Computations: A Spectral Method Approach*, Princeton University Press, 2010.

[6] B. A. Jones, Nathan Parrish, and Alireza Doostan, "Post-maneuver collision probability estimation using sparse polynomial chaos expansions," *Journal of Guidance, Control, and Dynamics*, vol. 36, no. 2, pp. 430–444, Mar.-Apr. 2014.

[7] B. A. Jones, A Doostan, and G.H. Born, "Nonlinear propagation of orbit uncertainty using non-intrusive polynomial chaos," *Journal of Guidance, Control, and Dynamics*, 2014, in press, available from: URL http: ccar.colorado.edubajonesfilesjones_2014a.pdf.

[8] B. A. Jones and A Doostan, "Satellite collision probability estimation using polynomial chaos expansions," *Advances in Space Research*, vol. 52, no. 11, pp. 1860–1875, 2013.

[9] J. T. Horwood, N. D. Aragon, and A. B. Poore, "Gaussian sum filters for space surveillance: Theory and simulations," *Journal of Guidance, Control, and Dynamics*, vol. 34, no. 6, pp. 1839–1851, 2011.

[10] Kyle J. DeMars, Robert H. Bishop, and Moriba K. Jah, "Entropy-based approach for uncertainty propagation of nonlinear dynamical systems," *Journal of Guidance, Control, and Dynamics*, vol. 36(4), pp. 1047–1057, 2013.

[11] Kyle J. DeMars, Yang Cheng, and Moriba K. Jah, "Making best use of model evaluations to compute sensitivity indices," *Journal of Guidance, Control, and Dynamics*, vol. 37(3), pp. 979–984, 2014.

[12] A. Doostan, A. Validi, and G. Iaccarino, "Non-intrusive low-rank separated approximation of high-dimensional stochastic models," *Computation Methods in Applied Mechanical Engineering*, vol. 263, pp. 42–55, 2013.

[13] Ryan S. Park and Daniel J. Scheeres, "Nonlinear mapping of gaussian statistics: Theory and applications to spacecraft trajectory design," *Journal of Guidance, Control, and Dynamics*, vol. 29, no. 6, pp. 1367–1375, 2006.

[14] K. Fujimoto, D. J. Scheeres, and K. T. Alfriend, "Analytical nonlinear propagation of uncertainty in the two-body problem," *Journal of Guidance, Control, and Dynamics*, vol. 35, no. 2, pp. 497–509, 2012.

[15] Manoranjan Majji, JohnL. Junkins, and JamesD. Turner, "A high order method for estimation of dynamic systems," *The Journal of the Astronautical Sciences*, vol. 56, no. 3, pp. 401–440, 2008.

[16] Martin Berz, *Differential Algebraic Techniques. Entry in Handbook of Accelerator Physics and Engineering*, World Scientific, New York, 1999a.

[17] Roberto Armellin and Francesco Topputo, "A sixth-order accurate scheme for solving two-point boundary value problems in astrodynamics," *Celestial Mechanics and Dynamical Astronomy*, vol. 96, no. 3-4, pp. 289–309, 2006.

[18] Roberto Armellin, Pierluigi Di Lizia, Franco Bernelli-Zazzera, and M Berz, "Asteroid close encounters characterization using differential algebra: the case of apophis," *Celestial Mechanics and Dynamical Astronomy*, vol. 107, no. 4, pp. 451–470, 2010.

[19] Roberto Armellin, Pierluigi Di Lizia, Francesco Topputo, Michele Lavagna, Franco Bernelli-Zazzera, and Martin Berz, "Gravity assist space pruning based on differential algebra," *Celestial mechanics and dynamical astronomy*, vol. 106, no. 1, pp. 1–24, 2010.

[20] Andrea Saltelli, Stefano Tarantola, Francesca Campolongo, and Marco Ratto, *Sensitivity Analysis in Practice: A guide to assessing scientific models*, Wiley, Hoboken, NJ, 2004.

[21] G. Blatman and B. Sudret, "Efficient computation of global sensitivity indices using sparse polynomial chaos expansions," *Reliability Engineering and System Safety*, vol. 95, pp. 1216–1229, 2010.

[22] A. Doostan, G. Iaccarino, and N. Etemadi, "A least-squares approximation of high-dimensional uncertain systems," Tech. Rep. Annual Research Brief, Center for Turbulence Research, Stanford University, 2007.

[23] A. Doostan and G. Iaccarino, "A least-squares approximation of partial differential equations with high-dimensional random inputs," *Journal of Computational Physics*, vol. 228, no. 12, pp. 4332–4345, 2009.

[24] A. Nouy, "Proper generalized decompositions and separated representations for the numerical solution of high dimensional stochastic problems," *Archives of Computational Methods in Engineering*, vol. 17, pp. 403–434, 2010.

[25] B. N. Khoromskij and C. Schwab, "Tensor-structured galerkin approximation of parametric and stochastic elliptic pdes," *SIAM Journal on Scientific Computing*, vol. 33, pp. 364–385, 2010.

[26] M. Chevreuil, R. Lebrun, A. Nouy, and P. Rai, "A least-squares method for sparse low rank approximation of multivariate functions," *arXiv preprint arXiv:1305.0030*, 2013.

[27] Mohammad Hadigol, Alireza Doostan, Hermann G Matthies, and Rainer Niekamp, "Partitioned treatment of uncertainty in coupled domain problems: A separated representation approach," *Computer Methods in Applied Mechanics and Engineering*, vol. 274, pp. 103–124, 2014.

[28] Lorenzo Tamellini, Olivier Le Maitre, and Anthony Nouy, "Model reduction based on proper generalized decomposition for the stochastic steady incompressible navier-stokes equations," *SIAM Journal on Scientific Computing*, vol. 36, no. 3, pp. A1089–A1117, 2014.

[29] M. Reynolds, A. Doostan, and G. Beylkin, "Randomized alternating least squares for canonical tensor decompositions: Application to a pde with random data," *arXiv preprint arXiv:1510.01398*, 2015.

[30] Marc Balducci, Brandon A. Jones, and Alireza Doostan, "Orbit uncertainty propagation with separated representations," *AAS/AIAA Astrodynamics Specialist Conference*, 2013, Hilton Head, SC, August 11-15.

[31] Yifei Sun and Mrinal Kumar, "Uncertainty propagation in orbital mechanics via tensor decomposition," *Celestial Mechanics and Dynamical Astronomy*, pp. 1–26, 2015.

[32] Greg Beylkin, J Garcke, and M. J. Mohlenkamp, "Multivariate regression and machine learning with sums of separable functions," *SIAM Journal on Scientific Computing*, vol. 31, no. 3, pp. 1840–1857, 2009.

[33] Juliana Feldhacker, Brandon Jones, and Doostan Alireza, "Trajectory optimization under uncertainty for rendezvous in the crtbp," *AAS/AIAA Astrodynamics Specialist Conference*, 2016, Napa, CA, February 14-18.

[34] Marc Balducci, Brandon A. Jones, and Alireza Doostan, "Orbit uncertainty propagation with separated representations," *Under Review*, 2016.

[35] Dongbin Xiu and George Em Karniadakis, "The wiener–askey polynomial chaos for stochastic differential equations," *SIAM journal on scientific computing*, vol. 24, no. 2, pp. 619–644, 2002.

[36] Juliana D Feldhacker, Brandon A Jones, Alireza Doostan, and Jerrad Hampton, "Reduced cost mission design using surrogate models," *Advances in Space Research*, vol. 57, no. 2, pp. 588–603, 2016.

[37] Robert W Farquhar, David W Dunham, and James V McAdams, "Near shoemaker at eros- rendezvous, orbital operations, and a soft landing," *Advances in the Astronautical Sciences*, 2002.